

“Canode”: A conical partially magnetic anode for efficient negative ion extraction from duoplasmatron ion sources

Ru”Canode”: duoplasmatron negative ion source

Running Authors: Williams et al.

Peter Williams^{1a}, Maitrayee Bose², Richard L. Hervig², Larry Nittler², Lynda B. Williams²

¹School of Molecular Sciences, Arizona State University, Tempe, AZ 85287

²School of Earth and Space Exploration, Arizona State University, Tempe, AZ 85287

a) Electronic mail: pw@asu.edu

We report on the design and performance of an improved duoplasmatron ion source for secondary ion mass spectrometers. The source is designed specifically to optimize extraction of negative oxygen ions while suppressing electron extraction using a built-in magnetic asymmetry in the anode electrode. Other changes from conventional designs are: (a) drilling the ion extraction aperture directly into the magnetic steel anode rather than in a refractory (non-magnetic) metal insert, thereby eliminating a magnetic “hole” that acts to counter the desired magnetic concentration of the discharge at the aperture, (b) forming the anode into a conical shape convex toward the intermediate electrode to increase the magnetic field concentration at the extraction aperture, hence the term “Canode”. The built-in magnetic asymmetry allows the width and shape of the intermediate electrode to be varied to further optimize magnetic concentration of the discharge. Tests were performed with both ims 6f and NanoSIMS 50L instruments manufactured by Cameca Instruments Inc. (Fitchburg, WI, USA). In the ims 6f, the

Canode design gave O^- primary ion currents up to a factor of five greater than the factory ion source design. In the NanoSIMS 50L the Canode source produced a focused O^- ion beam at the sample with a diameter of 50 nm, identical to the performance of the radio-frequency Hyperion ion source developed by Oregon Physics (Beaverton, OR, USA) and offered as an option by Cameca.

I. INTRODUCTION

The duoplasmatron is a high brightness gas discharge ion source widely used as a primary ion source in secondary ion mass spectrometers, and also to generate ions for particle accelerators. It was first described by Manfred von Ardenne in a 1956 treatise¹. The basic concept is a glow discharge, between a cathode and an anode, that is constrained to pass through an aperture in an intermediate, or *zwischen* (“Z”) electrode. An additional level of constraint is achieved by making the Z-electrode and the anode two poles of a magnetic circuit. The magnetic lines of force emanating from the interior of the aperture in the Z-electrode initially concentrate towards the central axis of the discharge and further concentrate the electrons, and thus the discharge, towards the axis. In the 1960’s, demand arose for an ion source that produced *negative* ions, initially for tandem Van de Graaff accelerators. These accelerators achieve final ion energies of at least twice that of a normal Van de Graaff by initially accelerating negative ions from near ground potential and then, in the high voltage terminal, passing the ions through a gas stripper cell to remove at least two electrons (converting H^- to H^+) or more (e.g. from C^- , C^{3+} can be produced). The resulting positive ions are then accelerated back down to

ground potential, achieving final energies higher than the initial energy in the high voltage terminal by a factor equal to the total change in charge, i.e. $2\times$ for H^-/H^+ or $4\times$ for C^-/C^{3+} . An additional demand for a negative oxygen ion source has arisen in secondary ion mass spectrometry (SIMS) instruments which utilize oxygen primary ions to enhance secondary positive ion yields. Initially, negative primary ions were used in SIMS to control sample charging in the analysis of insulating samples: negative ion impact tends to give a secondary electron yield >1 , so that the charging effect of the primary ions is countered. More recently, the development of the NanoSIMS instrument, initially designed by Prof. Georges Slodzian (University of Paris) and then commercialized by Cameca, made a negative primary ion source essential since in this instrument positive secondary ions are accelerated away from the sample through the same lens that focuses the incident primary ions, so the ion polarities must be opposite in sign and negative primary oxygen ions are required.

A significant problem in extracting negative ions from a duoplasmatron ion source is the much greater density of electrons in the gas discharge, leading to an extracted electron current that can be as much as 3 orders of magnitude greater than the negative ion current. This could place an excessive load on the accelerating voltage supply. In an influential paper in 1965, Lawrence and colleagues² introduced a novel design feature in the form of a laterally moveable Z-electrode. Using a discharge in H_2 gas and extracting H^- , these authors found that with a discharge current of 2 A and the Z-electrode coaxial with the extraction aperture the extracted electron current measured as a load at the grounded extraction electrode was as high as ~ 0.25 A and no extracted H^- could be detected beyond a downstream Wien filter intended to separate the electron and

ion currents. However, if the Z-electrode was translated laterally with respect to the extraction aperture, the electron current dropped almost to zero and the H^- current rose (to a maximum of $\sim 75 \mu A$). Similar results were obtained in a paper published a few months after that of Lawrence by Collins and Gobbett³. In discussing their findings, both sets of authors theorized that the negative ions in the discharge were concentrated toward the edge of the discharge which was presumed to be “cooler”. This concept has persisted to the present day.

The suggestion that the highest density of negative ions should be found at the periphery of the discharge leads to the obvious thought that instead of a movable Z-electrode, ions should be extracted through an annular slit aligned with the periphery of the Z-electrode aperture. In this case, the Z-electrode would not need to be displaced from the source axis. However, attempts to do this at General Ionex Corporation in the 1970s, using a set of small apertures drilled around the annulus to approximate a completely annular slit, produced little or no extracted negative ion current. This yielded the insight that the effect of displacing the magnetic Z-electrode must simply be to introduce an asymmetry into the magnetic field that suppresses electron extraction from the source and thus minimizes the drain on the high voltage power supply⁴. In the Lawrence paper, the ion source potential was stated to be -20 kV, so that an extracted electron current of 0.25 A would have required the high voltage power supply to have an unusually high power rating of at least 5 kW. If the power supply voltage dropped due to the electron current drain then the H^- ion energies would have been incorrect for passage through the downstream Wien filter.

The invention discussed in the present paper was aimed at modifying the factory duoplasmatrons used in the Cameca NanoSIMS 50L and ims 6f secondary ion mass spectrometry (SIMS) instruments at Arizona State University (ASU) to allow extraction of negative ions from the intense *central* region of the duoplasmatron discharge.

II. DESIGN CHANGES

A *Magnetic asymmetry*

The major design change was to *build in* a magnetic field asymmetry to deflect and suppress electron extraction by fabricating a portion of the anode from non-magnetic stainless steel. This asymmetry was achieved by fabricating the steel anode out of magnetic (mild steel) and non-magnetic (321 stainless steel) bars, brazed together and then machined into a circular shape with the magnetic/non-magnetic join offset laterally from the center.

Several additional changes were made to the conventional duoplasmatron design. Two changes were aimed at concentrating the magnetic field – and the discharge – at the anode aperture.

B *Anode aperture*

In the duoplasmatron as supplied by Cameca the 400 μm diameter anode aperture is drilled through a molybdenum disc insert, press-fitted into a ~ 3 mm diameter hole in the mild steel anode. The purpose of the molybdenum is presumably to make the aperture region more temperature-resistant. But the deleterious effect of this non-magnetic insert is to create a magnetic “hole” in the anode. Magnetic field lines that should concentrate near the aperture instead diverge to the periphery of this magnetic hole, countering the

focusing effect of the initially convergent field. In the present design, the anode aperture is drilled directly into the magnetic mild steel, with no insert. The lifetime of the mild steel apertures appears comparable to that of the molybdenum inserts: for example, the 6f Canode aperture imaged later in Fig. 9 had been in regular use for over a year and shows little degradation other than a small increase in diameter that does not appear to affect performance. We have fabricated replaceable (i.e. screw-in) conical mild steel aperture inserts in the event that aperture erosion becomes an issue.

C Anode geometry

In the duoplasmatron designs discussed in the literature and supplied with Cameca SIMS instruments, the rear of the magnetic anode facing the Z-electrode is flat and thus devoid of any focusing effect on the discharge electrons. In the present design the rear of the anode is given a shallow conical shape to maximize magnetic field intensity at the aperture. This conical anode⁵ has been given the name “Canode” (L.B. Williams, ASU).

D Z-electrode geometry

Given that the need to align the extraction aperture with the edge of the Z-electrode was eliminated, a final design change was to alter the geometry of the Z-electrode to increase the electron focusing strength of the magnetic field at the Z-electrode aperture.

The initial Canode design is shown in Fig. 1. Also shown in Fig. 1 is the initial manufacturer-supplied Z electrode (top) which, for the NanoSIMS instrument, we modify slightly by fabricating a shallow recess on the top side of the aperture to capture nickel oxide debris from the hollow cathode that otherwise can fall down the vertical primary ion column and cause contamination. This minor design change reduces the need to

disassemble and clean the ion source and significantly extends the source lifetime between cleanings.

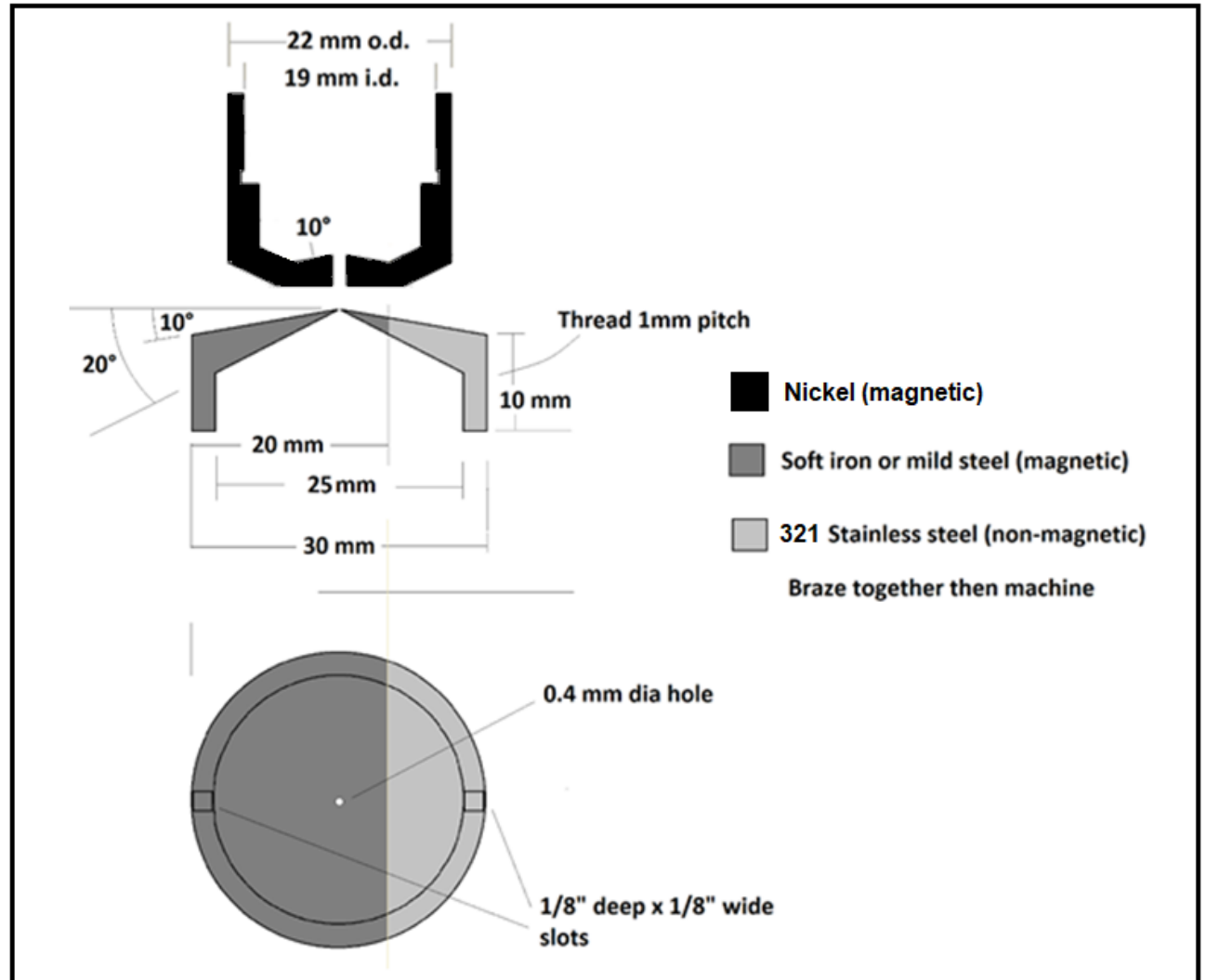


Fig. 1. Design of the Canode. **Upper:** Cross-section through the center of the Canode and Z-electrode. **Lower:** Bottom-view of the Canode as shown in the top image. The two slots in the rim are for a tool to aid in screwing the Canode into the anode plate.

III. PERFORMANCE AND TESTING: FACTORY Z-ELECTRODE

The Canode design has been evaluated on the Cameca ims 6f and NanoSIMS 50L instruments at Arizona State University. Initial tests used the Z-electrode aperture dimensions as supplied by Cameca, 1.5 mm diameter, 3 mm long, with the minor change shown in Fig. 1 of adding a shallow debris capture groove for the NanoSIMS Z-electrode.

Using the ims 6f, we find that the Z-electrode positions to optimize both O_2^+ and O^- primary ion currents are now roughly similar, in comparison to the factory source for which the negative ion optimum is offset sideways by roughly 0.5 Z-electrode aperture widths (~ 0.7 mm for the factory design) from the axial positive ion position. However, due to the built-in magnetic asymmetry this optimum position is now off-axis for both ion polarities.

A. *Primary beam stability*

For reasons not fully understood, in the ims 6f the Canode O^- primary ion currents appear to be distinctly more stable than currents from the factory duoplasmatron. Figure 2 shows secondary ion signals for $^{28}Si^+$ sputtered from a silicon wafer over a period of almost 50 minutes using an 11 nA O_2^- primary beam at 17.5 keV impact energy. The maximum and minimum data points in the plot differ by 3.9%. The standard deviation of the entire data set of Fig. 2 was 0.8%.

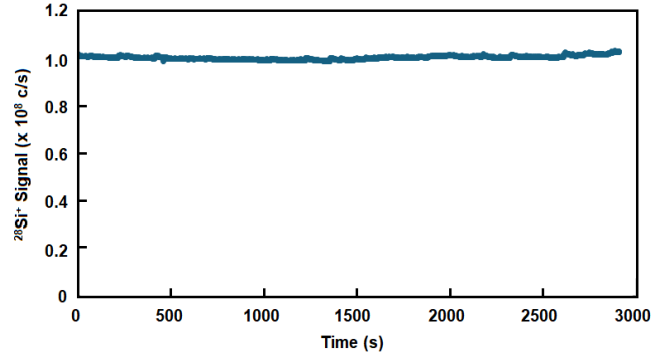


Fig. 2. Stability data for Si^+ sputtered from a silicon wafer over a 50 minute period

B. Primary ion currents

Using a Canode with a 600 μm diameter ion extraction aperture mounted in the ims 6f duoplasmatron (and all other primary ion column parameters remaining the same as for the factory source), the following primary ion currents were achieved:

TABLE I. Maximum currents obtained with the Canode source design on our Cameca ims 6f instrument compared to the factory design. The Z-electrode was the same factory design (1.5 mm i.d.) for both. The Canode aperture diameter was 0.6 mm.

	O_2^+	O^-	O_2^-	m/z 48 ⁻ (b)
Max. Current (Canode)	> 6 μA	> 5 μA	2.6 μA	~ 800 nA
Max. current (Cameca source)	~ 1-2 μA	~ 1 μA	(a)	~200-300 nA

Notes:

- (a) We did not examine the O_2^- primary species with the Cameca duoplasmatron and Cameca does not cite a primary current specification for this species

(b) Note that the m/z 48 species in the ims 6f appears to be significantly contaminated by NO_2^- , as indicated by depth profiles into N-implanted minerals revealing significant N^+ signals, overwhelming the implant (which was observed as normal if the O_2^- primary species was used). Additionally, comparison of Si^+ signals from a silicon sample sputtered by identical primary currents of m/z 16, 32 and 48 species showed a scaling of $\sim 1 : 2.3 : 1.6$ rather than the anticipated scaling of $\sim 1 : 2 : 3$. The possibility of a small air leak introducing nitrogen into the ims 6f ion source cannot be ruled out. We have observed no evidence for NO_2^- contamination of the m/z 48 species in the NanoSIMS work discussed later. Work is continuing to determine the composition and origin of the m/z 48 primary species in the ims 6f.

The improved current value for O_2^+ in addition to the negative ion improvements is gratifying and may reflect the improved magnetic focusing of the discharge at the extraction aperture due to the conical Canode shape and the elimination of the magnetic “hole” due to the molybdenum insert.

C. Primary ion beam focusing: factory Z-electrode

O^- ion beam focusing for the design of Fig. 1 was evaluated on the NanoSIMS instrument using a spatial resolution test sample supplied by Cameca. The test sample was a slurry of finely-ground SiO_2 particles in molten aluminum, solidified, cut and polished. Fig. 3 shows data obtained using the Canode with the factory Z-electrode.

Fig. 3(a) shows an image of the test sample using $^{27}\text{Al}^+$ secondary ions. The line scan shown in Fig 3(b) was obtained normal to a sharp edge in the upper left quadrant of the image (labeled “1” by the NanoSIMS software) and was used to calculate the beam size. Assuming a Gaussian beam shape, the distance from 16% to 84% amplitudes

corresponds to ± 1 standard deviation of the beam width and was found to be 76 nm. The O^- current at the sample Faraday cup was 0.3 pA. Slits in the secondary mass

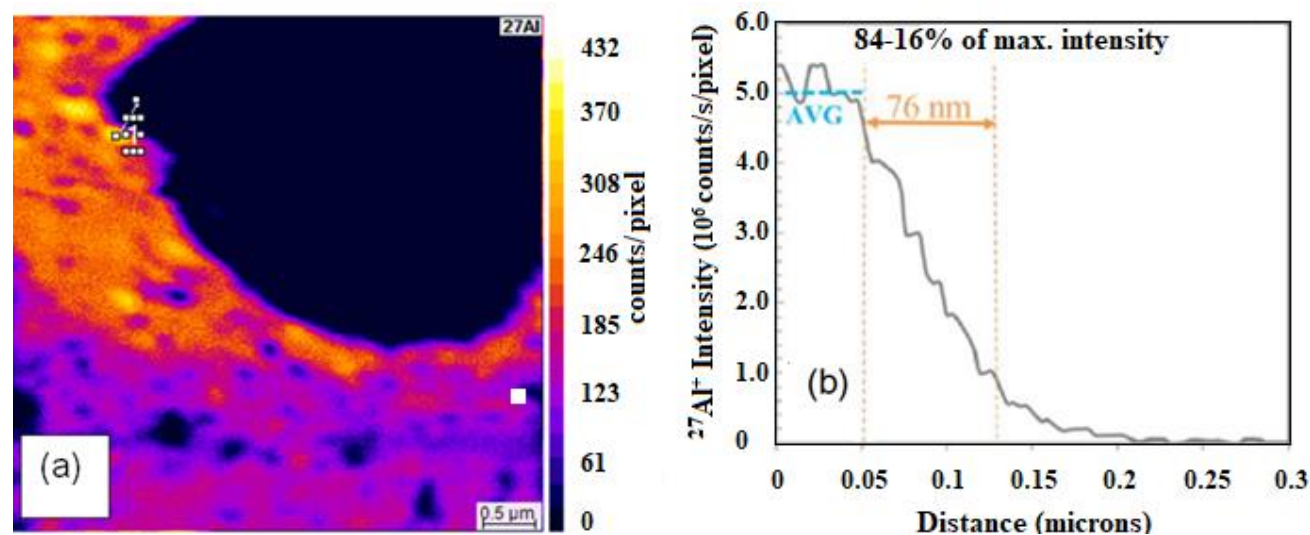


Fig. 3. Initial beam size data with the Canode design showing the 76 nm beam size with 0.3 pA current. The factory Z-electrode was used (1.5 mm diameter x 3 mm length).

- (a) Image of a feature in the Cameca test sample. The line scan was obtained across the edge of a sharp feature in the upper left quadrant (partially obscured by the label “1”)
- (b) $^{27}\text{Al}^+$ intensity along the line scan showing a beam width of 76 nm.

spectrometer of the NanoSIMS were wide open to maximize secondary ion transmission and signal strength for the low primary beam currents. This is the normal operating condition used by Cameca in determining beam size data for the factory ion sources: note that the secondary ion transmission has no direct effect on the primary beam performance other than to increase the signals detected for low primary beam currents. The performance shown in Fig. 3 is a significant improvement over the factory specification for the unmodified duoplasmatron which is: 400 nm beam diameter at 2 pA O^- current

and a minimum beam diameter of 200 nm (current not specified but presumably $\sim 0.2 - 0.3$ pA).

IV. PERFORMANCE AND TESTING: EFFECT OF Z-ELECTRODE GEOMETRY

The final design change involved evaluating the effect of changing the Z-electrode geometry from the factory design. One reason for the aperture diameter of 1.5 mm in the factory design was that the lateral motion of the Z-electrode is limited to about a 2 mm range, thus if it is desired to align the edge of the Z-electrode aperture with the anode aperture, the Z-electrode aperture diameter should be less than ~ 2 mm. Given that we now have a different mechanism to suppress electron extraction we are now free to explore different Z-electrode geometries.

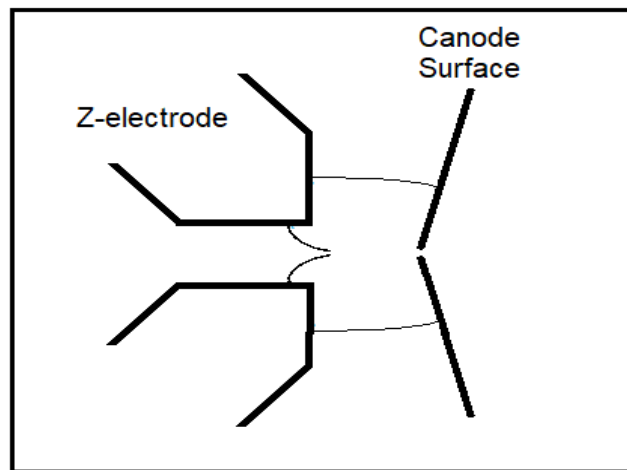


Fig. 4. Depiction of magnetic lines of force between the Z-electrode and the Canode surface.

Fig. 4 indicates the shape of the magnetic field between the Z-electrode and the Canode surface. Magnetic field lines of force have two fundamental properties that are essential to the present discussion: (a) initially the lines of force are perpendicular to the surface from which they issue, and (b) lines of force can never cross each other. This leads to the field shape shown in the interior of the Z-electrode aperture, where the lines of force initially converge and then curve together. This shape can produce a strong converging effect on electrons in the discharge, and a significantly weaker (arguably negligible) effect on the much more massive ions. It is easy to argue that the strength of this focusing effect is dependent on the Z-electrode aperture size (and shape). Consider a situation where we make the Z-electrode aperture vanishingly narrow. In this case the Z-electrode surface is effectively flat and the magnetic focusing effect disappears. Thus, we chose to explore the effect of changing the Z-electrode aperture shape to increase the magnetic focusing effect⁶. The initial change was to make the aperture *larger* than the factory diameter of 1.5 mm. The aperture tested was a cylindrical shape with 4 mm internal diameter, shown in Fig. 5.

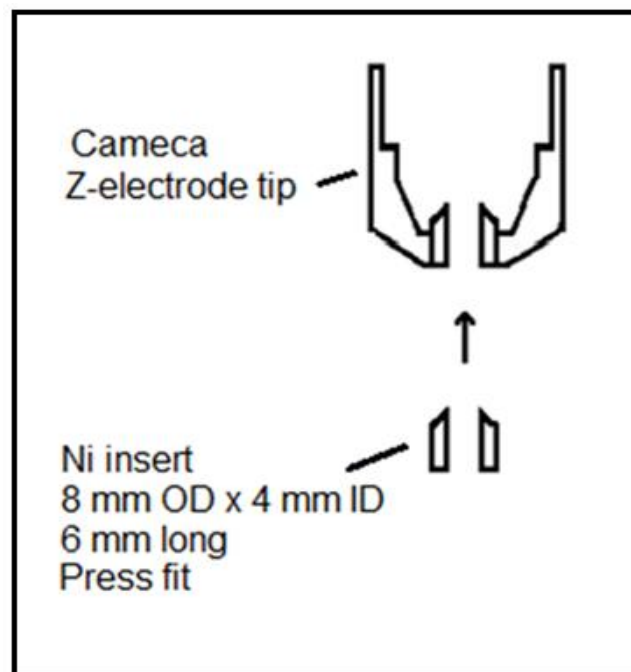


Fig. 5. Widened Z-electrode aperture.

The Z-electrode modification shown in Fig. 5 was made by drilling out the existing aperture in the screw-on tip of a nickel Z-electrode and press-fitting a new nickel aperture with internal diameter 4 mm and length 8 mm (this 2:1 ratio of aperture length to diameter was recommended in an exhaustive study of duoplasmatron parameters by Lejeune⁷). The internal protrusion of the aperture piece again generates a trap for falling hollow cathode debris in the vertical NanoSIMS primary ion column. The performance of the Canode with this enlarged aperture was initially evaluated by Cameca North America service engineer Jianchao Zhang during a service visit. No ASU personnel were present during this test. With the O⁻ beam apertured and focused down to a current of ~0.1 – 0.2 pA at the sample, a beam diameter of 50 nm was achieved (Fig. 6). Two independent

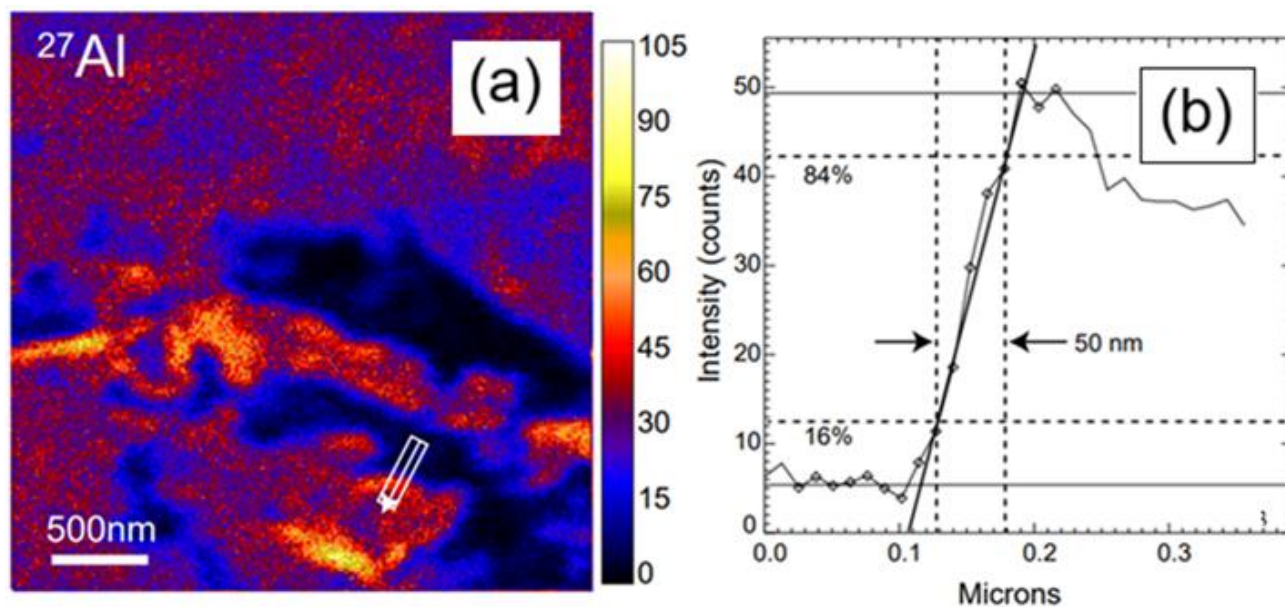


Fig. 6 (a) Image of test sample using the Canode source with a 4 mm diameter Z-electrode aperture (Jianchao Zhang, Cameca). A line scan was obtained at the position indicated below and to the right of center. (b) Line scan data processed in L'Image

software (L. Nittler) indicating a primary beam diameter of 50 nm. (The intensity values shown are counts/pixel.)

beam size measurements using the scan in Fig 6 were performed by engineer Zhang using the Cameca WinImage software and by co-author Nittler using his proprietary L'Image software (Fig. 6b), giving results of 51 nm and 50 nm respectively.

In enlarging the Z-electrode aperture we sacrificed the other claimed property of the Z-electrode, namely a mechanical constriction of the discharge. The next geometry we explored was an attempt to combine mechanical constriction with strong magnetic focusing. The initial design for this is shown in Fig. 7. The aperture shape in Fig 7 was made by simply taking a standard Z-electrode tip with a 1.5 mm internal diameter and machining a 45° bevel into the lower 50% of the channel as shown. The initial part of the channel imposes a mechanical constriction on the discharge and then the magnetic lines

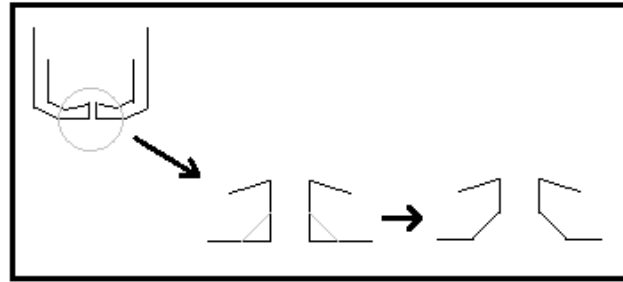


Fig. 7. Z-electrode electrode geometry combining mechanical and magnetic constriction.

of force from the bevel surface again converge to produce a stronger focusing effect than that from field penetration in the full-length narrow channel. A particular hope for the beveled aperture design was that forcing the discharge through the narrow part of the

aperture might increase ion-molecule collisions that produce O_3^- . O_3^- is a desirable primary ion species for SIMS because, for a given primary ion current density, sputtering and signal acquisition rates should be $\sim 3\times$ faster than for O^- , while ionization probabilities should be roughly comparable⁸. An additional advantage over O^- is that depth resolution should be $3\times$ better for a given impact energy because fragmentation upon impact with the sample surface results in three atomic projectiles initially with the same velocity as the triatomic projectile and thus with $1/3$ the energy and penetration depth.

The beveled channel design was tested by co-author Nittler for its performance for O_3^- production, in a search for isotopically anomalous pre-solar grains in a meteorite (Acfer 094)⁹. The images of Fig. 8 show very encouraging O_3^- performance: the measured beam diameter was 70 nm (a and b) with an O_3^- beam current at the sample of 1 pA. It should be noted also that these images were obtained with a secondary ion mass resolving power of $\sim 3,000 - 5,000$, i.e. realistic operating conditions as shown by the Mg-isotopic images of a presolar grain in a meteorite (c and d). This beam was judged by Nittler to provide very similar resolution and secondary ion count rates to that of a 2-3 pA O^- beam generated by a Hyperion RF source on the NanoSIMS 50L at the Carnegie Institution for Science.

(Following up on the earlier discussion of Table 1 concerning possible contamination of the m/z 48 primary beam in the ims 6f by NO_2^- , we note that unlike the ims 6f results the secondary ion yields in the NanoSIMS using the m/z 48 primary beam were approximately $3x$ the O^- yields, as would be expected for an O_3^- beam.)

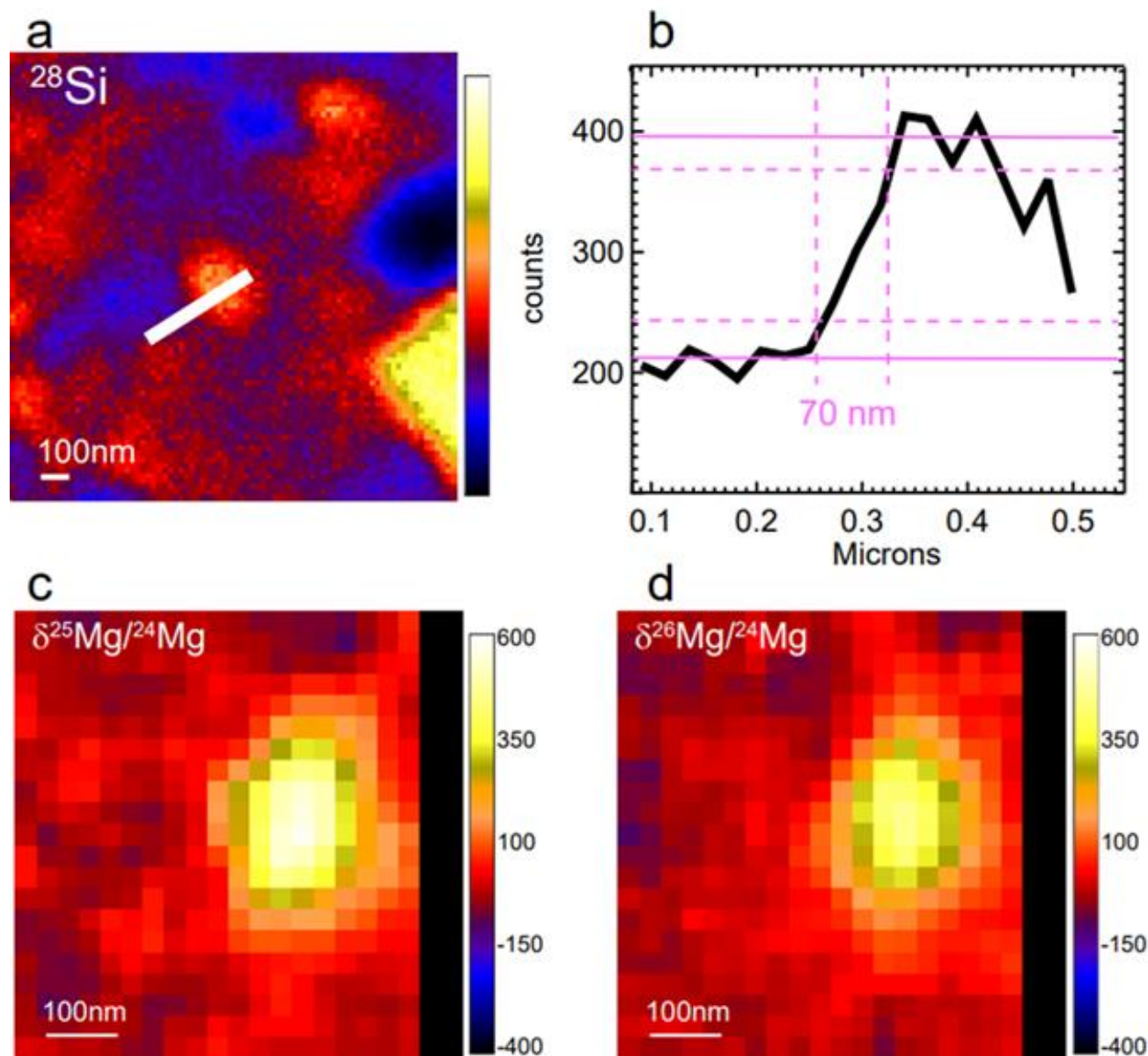


Fig. 8. **a)** ^{28}Si image of a small portion of the Acfer 094 meteorite sputtered with an O_3^- primary beam; the white line indicates the profile across a Si-rich particle. **b)** The line profile from (a) indicates a beam size of 70nm. **c)** and **d)** Mg-isotopic ratio images, expressed as part-per-thousand deviations from terrestrial values ($\delta^{25}\text{Mg}/^{24}\text{Mg}$, $\delta^{26}\text{Mg}/^{24}\text{Mg}$) revealing a small, highly isotopically anomalous presolar grain. Images were acquired with the beveled Z-electrode aperture and a 1-pA (nominal) O_3^- primary beam.

V. Z-ELECTRODE POSITIONING

As discussed, the magnetic field asymmetry introduced by the partially non-magnetic construction of the Canode clearly serves to suppress electron extraction and to allow ion extraction from a significantly more intense region of the discharge. However, particularly with the enlarged and/or reconfigured Z-electrode apertures discussed in part IV above, it was noticeable that the lateral position of the Z-electrode still needed to be off-center for optimum negative ion performance. A clue to this behavior came from examining the electron burn marks on the interior surfaces of used Canodes, shown in Figure 9.

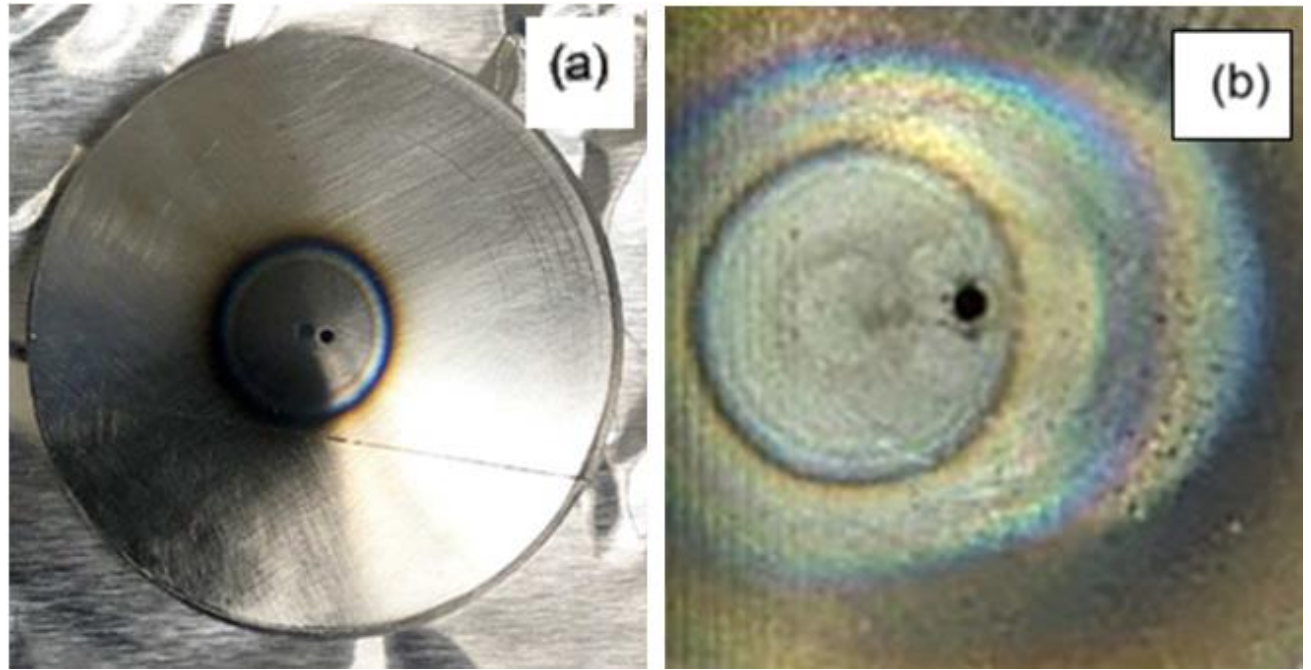


Figure 9. (a) Electron burn mark on the interior surface of a Canode from the ims 6f. Full diameter of the Canode is 30 mm. The aperture diameter is $\sim 800 \mu\text{m}$. (b) Electron burn marks on the interior surface of a multiply-used Canode from the NanoSIMS. Full diameter of the Canode was the same as in Fig. 9 (a). The aperture diameter is $400 \mu\text{m}$.

Figure 9(a) shows the interior surface of a used Canode from the ims 6f. This Canode had been used in our ims 6f instrument over more than a year without any change in orientation or spacing and had an aperture diameter that had increased from its initial value of 600 μm to almost 800 μm . The image was obtained after a few weeks of use following cleaning of the part. The Z-electrode in this case was the original Cameca piece with a 1.5 mm aperture diameter. The magnetic/non-magnetic join is visible below the central aperture with the non-magnetic portion in the lower part of the image; the join is slightly off horizontal in the image (tilted slightly down left to right). The large oxidation circle (~ 12 mm diameter) resulted from electron beam bombardment and heating in the oxygen gas in the source. The ion extraction aperture is the small dark feature to the right of the center of this oxidation circle. The burn mark made by the focused electron beam is visible at the center of the oxidation circle to the left of, and slightly above, the aperture. Using the aperture diameter as a length scale, the electron beam diameter in this image appears to be $\sim 800\text{-}900$ μm , i.e. there is some degree of electron focusing by the 1.5 mm diameter Z-electrode aperture. Note again that the magnetic field orientation is always perpendicular to the magnetic/non-magnetic join and so the electron deflection is therefore parallel to the direction of the join. Figure 9(b) shows electron burn marks on the interior of a Canode used over an extended period in the NanoSIMS instrument with an enlarged Z-electrode aperture for stronger electron focusing. Multiple burn marks are visible because this Canode had been used to explore several different distance settings from the Z-electrode, achieved by screwing the Canode towards or away from the Z-electrode in $\frac{1}{2}$ -turn increments (i.e. keeping the magnetic/non-magnetic join parallel to the Z-electrode motion). One weak burn mark to

the right of the aperture corresponds to the magnetic/non-magnetic join having been rotated 180° from the orientations producing the burn marks to the left of the aperture. The aperture diameter for this Canode was $400\ \mu\text{m}$; two small electron burn marks to the left of the aperture indicate electron beam diameters smaller than $400\ \mu\text{m}$, consistent with the improved ion currents obtained with the stronger focusing enlarged Z-electrode aperture.

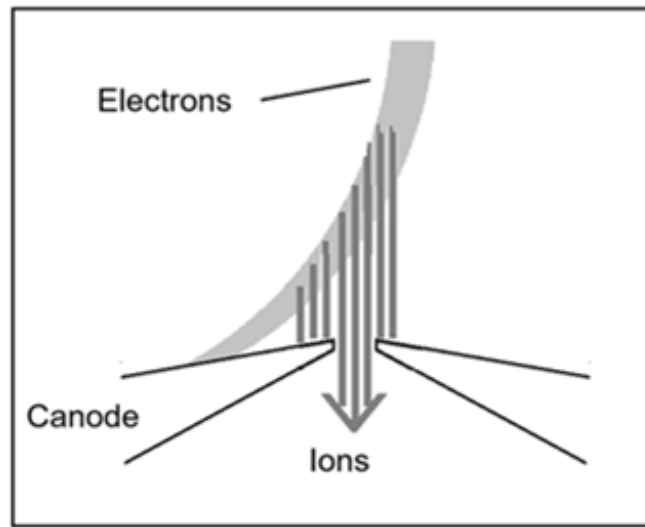


Figure 10. Sketch of presumed electron and ion trajectories.

Figure 10 is a sketch to explain the Z-electrode positioning and burn marks. Clearly the electrons are deflected sideways away from the extraction aperture by the built-in magnetic asymmetry, as intended. Clearly, also, the negative ions are far too massive to be affected by magnetic fields that cause the electron deflection that is observed, but ions can only be formed in the discharge along the electron path. The conclusion is that the extracted negative ions must have been formed within a few mean free path distances (on the order of a millimeter) of the aperture, at a position where the electrons have already

been deflected off the central axis of the Z-electrode so that the Z-electrode must be displaced sideways to align this ion origin region with the extraction aperture. The ion currents (few μA) are much weaker than the electron currents (50 - 100 mA) and so do not contribute to the burn mark.

In comparing our data with the performance for the Hyperion RF primary ion source offered as an option by the NanoSIMS manufacturer we note these features:

- a) The 50 nm beam diameter specification for the RF source is achieved for a minimal beam current that is typically around 0.2 pA or less, similar to our data in Fig. 6
- b) Although not stated by Cameca, it is understood that the RF source specification is achieved with the instrument slits wide open (giving greater transmission and enabling operation at low primary beam current), again similar to our operating conditions for Fig. 6
- c) As noted earlier, the spatial resolution and measured count rates for the images reported in Fig. 8 were closely similar to those previously obtained by co-author Nittler on similar samples with a 2-3 pA O^- beam generated by the Hyperion RF plasma source on the NanoSIMS 50L at the Carnegie Institution for Science.

VI. CONCLUSIONS

Work with the Canode disproves the 60 year-old conjecture^{2,3} that negative ions survive better at the edge of the discharge through the Z-electrode and seems to confirm the suggestion⁴ that the effect of an offset Z-electrode is simply to introduce a magnetic field asymmetry that suppresses electron extraction. Maximum currents, of both positive (O_2^+) and negative (O^-) oxygen ions with the Canode design are at least a factor of 5

higher than from the Cameca factory duoplasmatron design, consistent with ion extraction from the more intense central region of the discharge. However, this “central” region follows the electrons that are displaced sideways by the transverse magnetic field, so that Z-electrode displacement is still required to align the ion-forming region with the axial ion extraction aperture. O_3^- currents in the NanoSIMS appear sufficiently intense to make this species a useful alternative to the other negative oxygen species. Minimum O^- beam sizes obtained to date in the NanoSIMS appear identical to those obtained with the Hyperion radio-frequency source produced by Oregon Physics LLC and offered as an option by Camecac. One parameter that has yet to be explored is the arc discharge current. In a design decision dating back to the earliest Cameca ims 3f instruments produced in the 1970s (or possibly even earlier), the arc current in the Cameca duoplasmatron is limited to no more than 99 mA. The arc voltage is not displayed as a parameter but measurements on our duoplasmatron operating at 99 mA arc current (and a low accelerating voltage!) showed an arc voltage (cathode – anode) of 347 V, dropping slightly to 341 V at 50 mA arc current. Doubling the pressure reduced the arc voltage to 331 V at 99 mA arc current. So the maximum duoplasmatron power is roughly 35 W, compared to 800 W in the Hyperion source. We note that in the early duoplasmatron studies in references 2 and 3, arc currents were 2 A and up to 10 A (!) respectively. It would be extremely interesting to explore the effect of a simple modification of software and/or hardware to allow an increase in the arc current in the Canode duoplasmatron that should result in an increased ion current. It seems possible that focused beam sizes significantly smaller than 50 nm may be achievable in the NanoSIMS given a larger initial primary ion current. In addition, larger primary currents should enable faster

analyses, for a given beam size, in all of the Cameca instrument line. Finally, the duoplasmatron studies of references 2 and 3 were aimed at H⁻ production for tandem Van de Graaff accelerators. To the extent that these accelerators still utilize duoplasmatron ion sources, it seems useful to explore the utility of the Canode design for this application also.

Acknowledgements

As noted, the beam size data shown in Fig. 6 were obtained by Jianchao Zhang (Cameca) during a service visit; his skill is greatly appreciated. The expertise of machinists John Prince and William Chapin was invaluable, as is the advice and support of Dr. K. Amanda Williams. We are grateful to the U.S. National Science Foundation for supporting the operation of the ASU SIMS and NanoSIMS instruments as a multi-user community facility since 2009. This work was supported by NSF Grant EAR 1819550 (R.L. Hervig, PI).

Data availability: The data that support the findings of this study are available within the article.

Author declarations:

Conflict of interest: The authors have no conflicts to disclose.

Literature cited

- ¹M. von Ardenne *Tabellen der Elektronenphysik, Ionenphysik und Übermikroskopie. Bd. 1. Hauptgebiete* (VEB Dt. Verl. d. Wissenschaften, 1956)
- ²G.P. Lawrence, R.K. Beauchamp, J.L. McKibben, *Nucl. Instr. Methods* **32**, 357 (1965)
- ³L.E. Collins, R.H. Gobbett, *Nucl. Instr. Methods* **35**, 277 (1965)

This is the author's peer reviewed, accepted manuscript. However, the online version of record will be different from this version once it has been copyedited and typeset.
PLEASE CITE THIS ARTICLE AS DOI: 10.1116/6.0004627

⁴P. Hanley, General Ionex Corp. Personal Communication to PW

⁵P. Williams, US Patent No. 11,289,299 (29 March 2022)

⁶P. Williams, US Patent pending, submitted July 25, 2024

⁷C. Lejeune, Nucl. Instr. Methods **116**, 429 (1974)

⁸E. E. Groopman, T. L. Williamson, D. S. Simons, J. Anal. At. Spectrom. **37**, 2089
(2022)

⁹L.R. Nittler, C. Kraver, M. Bose, and P. Williams, 86th Annual Meeting of the
Meteoritical Society, (2024), Abstract #6465